




Developing urinary pyrrole–amino acid adducts as non-invasive biomarkers for identifying pyrrolizidine alkaloids-induced liver injury in human

Lin Zhu¹ · Chunyuan Zhang¹ · Wei Zhang² · Qingsu Xia³ · Jiang Ma¹ · Xin He¹ · Yisheng He¹ · Peter P. Fu³ · Wei Jia⁴ · Yuzheng Zhuge² · Ge Lin¹ 

Received: 17 May 2021 / Accepted: 29 July 2021 / Published online: 14 August 2021
© The Author(s), under exclusive licence to Springer-Verlag GmbH Germany, part of Springer Nature 2021

Abstract

Pyrrolizidine alkaloids (PAs) have been found in over 6000 plants worldwide and represent the most common hepatotoxic phytotoxins. Currently, a definitive diagnostic method for PA-induced liver injury (PA-ILI) is lacking. In the present study, using a newly developed analytical method, we identified four pyrrole-amino acid adducts (PAAAs), namely pyrrole-7-cysteine, pyrrole-9-cysteine, pyrrole-9-histidine, and pyrrole-7-acetylcysteine, which are generated from reactive pyrrolic metabolites of PAs, in the urine of PA-treated male Sprague Dawley rats and PA-ILI patients. The elimination profiles, abundance, and persistence of PAAAs were systematically investigated first in PA-treated rat models via oral administration of retrorsine at a single dose of 40 mg/kg and multiple doses of 5 mg/kg/day for 14 consecutive days, confirming that these urinary excreted PAAAs were derived specifically from PA exposure. Moreover, we determined that these PAAAs were detected in ~82% (129/158) of urine samples collected from ~91% (58/64) of PA-ILI patients with pyrrole-7-cysteine and pyrrole-9-histidine detectable in urine samples collected at 3 months or longer times after hospital admission, indicating adequate persistence time for use as a clinical test. As direct evidence of PA exposure, we propose that PAAAs can be used as a biomarker of PA exposure and the measurement of urinary PAAAs could be used as a non-invasive test assisting the definitive diagnosis of PA-ILI in patients.

Keywords Hepatotoxicity · Pyrrolizidine alkaloids-induced liver injury · Pyrrole-amino acid adducts · Biomarker · Non-invasive

Introduction

Pyrrolizidine alkaloids (PAs) are a group of the most common phytotoxins that can produce toxicity in different organs, especially in the liver (He et al 2021a; Shrenk et al. 2020; Song et al. 2020). PAs and their corresponding *N*-oxides are widely present in about 3% of floriferous plants globally (Mattocks 1986). More than 660 potentially poisonous PAs and PA *N*-oxides have been identified in over 6000 plants (Fu et al. 2004; Yang et al. 2017). Humans are readily exposed to toxic PAs through the consumption of PA-producing plants used as herbal medicines, herbal teas, and dietary supplements (Edgar et al. 2015; Kakar et al. 2010), and PA-contaminated staple foods such as grains, milk, tea, and honey (Edgar et al. 1999; He et al. 2020; Kempf et al. 2010; Zhu et al. 2018). In humans, ingestion of PAs and PA *N*-oxides often results in liver injury, particularly the severe PA-induced liver injury (PA-ILI) can cause hepatic

Lin Zhu, Chunyuan Zhang, and Wei Zhang have contributed equally to this work.

✉ Yuzheng Zhuge
yuzheng9111963@aliyun.com

✉ Ge Lin
linge@cuhk.edu.hk

¹ School of Biomedical Sciences, Faculty of Medicine, The Chinese University of Hong Kong, Hong Kong SAR, China

² Department of Gastroenterology, Nanjing Drum Tower Hospital, The Affiliated Hospital of Nanjing University Medical School, Nanjing, China

³ National Center for Toxicological Research, Food and Drug Administration, Jefferson, AR 72079, USA

⁴ School of Chinese Medicine, Hong Kong Baptist University, Hong Kong SAR, China

sinusoidal obstruction syndrome (HSOS) with typical symptoms of hepatomegaly, jaundice, and ascites (Chojkier 2003; DeLeve et al. 1999). However, except for the severe injury with typical HSOS syndrome and higher mortality, the relatively less severe symptoms of PA-ILI can recapitulate clinicopathological features of several kinds of acute and chronic liver diseases, such as viral hepatitis, decompensated cirrhosis, and Budd–Chiari syndrome (BCS), etc., and thus, it presents a diagnostic challenge in clinic to confirm that the liver injury is due to PA exposure.

The first human PA-poisoning cases were reported in 1920 in South Africa with 11 individuals involved and death of the majority of them (Willmot et al. 1920). Since then, over 15,000 acute PA-poisoning cases with obvious clinical symptoms have been documented worldwide in many regions/countries, including Afghanistan, China, Germany, Hong Kong, India, Jamaica, South Africa, Switzerland, the United States, etc. (Lin et al. 2011; Ma et al. 2019; Ruan et al. 2015; Zhu et al. 2020). Nevertheless, the diagnosis of the majority of these reported poisoning cases was based on typical symptoms of HSOS with either known history of exposure to PA-producing herbs or PA-contaminated food-stuffs or through retrospective investigations to confirm the PA exposure. It is very likely that much more PA-ILI cases are unaware, and currently, the risk of PA-ILI has not been addressed appropriately. Therefore, it is highly needed to develop a reliable clinical test for specific diagnosis of PA-ILI via the definitive confirmation of PA exposure.

PAs are esters comprised of a necine base and one or two ester groups connected at the C7 and C9 positions of the necine base and are classified into three types: retronecine (including its 7- α -enantiomer), otonecine, and platynecine (Fig. 1). The former two types possessing unsaturated necine bases are highly hepatotoxic and genotoxic (Fu et al. 2004; Mattocks 1982). Retronecine-type PAs commonly co-exist with their corresponding *N*-oxides in plants (Cao et al. 2008; Molyneux et al. 2011; Williams et al. 2011; Yang et al. 2019, 2020). Toxic PAs and PA *N*-oxides are pro-toxins. Their metabolic activation, catalyzed by hepatic cytochrome P450 enzymes (CYPs), especially CYP3A4 isozyme, generates the reactive metabolites, dehydropyrrolizidine alkaloids (DHPAs). DHPAs are highly unstable and readily react with nearby constituents to form a series of secondary pyrrolic metabolites and pyrrolic adducts, such as: (a) reacting with water to generate the hydrolyzed product (\pm)-6,7-dihydro-7-hydroxy-1-hydroxymethyl-5*H*-pyrrolizine (DHP) as the most abundant detectable pyrrolic metabolite (Edgar et al. 2015; Fu et al. 2004; Mattocks 1986); (b) interacting with cellular proteins to form pyrrole-protein adducts (PPAs) (Edgar et al. 2015; Lin et al. 2011; Lu et al. 2018; Mattocks 1986; Ruan et al. 2015); (c) binding with glutathione (GSH) to generate pyrrole-GSH conjugates (Lin et al. 2000; Ma et al. 2015); (d) reacting with cellular amino

acids to form pyrrole-amino acid adducts (PAAAs) (He et al. 2016a, 2016b; Xia et al. 2018); and (e) binding with cellular DNA to form pyrrole-DNA adducts (He et al. 2021b; Xia et al. 2013; Zhu et al. 2017). The above-described pyrrolic adducts are also produced through reactions with the more long-lived hydrolysis product, DHP (Edgar et al. 2015; Fu 2017) (Fig. 1). All these pyrrolic adducts have been shown to be potentially responsible for PA-ILI and/or PA-induced liver tumor initiation. On the other hand, some of the aforementioned pyrrolic adducts undergo further degradation to generate PAAAs, which plus initially formed PAAAs via pathway (f) eventually excrete from urine (Fig. 1).

Previously, we have developed a specific pre-column derivatization method followed by ultra-high-performance liquid chromatography–tandem mass spectrometry (UHPLC–MS/MS) analysis to measure pyrrole–plasma protein adducts in both PA-treated experimental animals and PA-exposed human samples (Lin et al. 2011; Ruan et al. 2015; The USA Centers for Disease Control and Prevention (CDC) 2012; Yang et al. 2017). We further established pyrrole–hemoglobin adducts, another type of blood PPAs with the advantage of longer persistence in PA-ILI patients for the definitive test of PA exposure (Ma et al. 2019, 2020). However, the analysis of blood PPAs has the following drawbacks: (1) an invasive (or a quasi-non-invasive) sample collection procedure, and (2) the requirement of chemical degradation of PPAs into derivatives prior to the analysis. Therefore, in the present study, we developed a UHPLC–MS/MS analytical method for directly detecting 4 PAAAs in the urine of PA-treated rats and PA-ILI patients. We propose that these urinary PAAAs can be used as a novel non-invasive biomarker for assisting the definitive diagnosis of PA-ILI in the clinic.

Experimental section

Chemicals

Retrorsine (RTS) and monocrotaline were purchased from Sigma-Aldrich (St. Louis, MO, USA). Ketamine and xylazine were obtained from Alfasan (Woerden, Holland). Four PAAA standards, namely pyrrole-7-cysteine, pyrrole-9-cysteine, pyrrole-9-histidine, and pyrrole-7-acetylcysteine, were synthesized by our group as reported previously (He et al. 2016a, b; Ma et al. 2019; Zhao et al. 2011, 2012). Briefly, monocrotaline was reacted with *o*-chloranil to produce dehydromonocrotaline, which was reacted individually with cysteine, histidine, or *N*-acetylcysteine, to generate pyrrole-7-cysteine, pyrrole-9-cysteine, pyrrole-9-histidine, and pyrrole-7-acetylcysteine. Each of the synthesized PAAA was purified from the reaction mixture and their structures were confirmed by MS and NMR spectroscopy. All solvents used were HPLC grade.

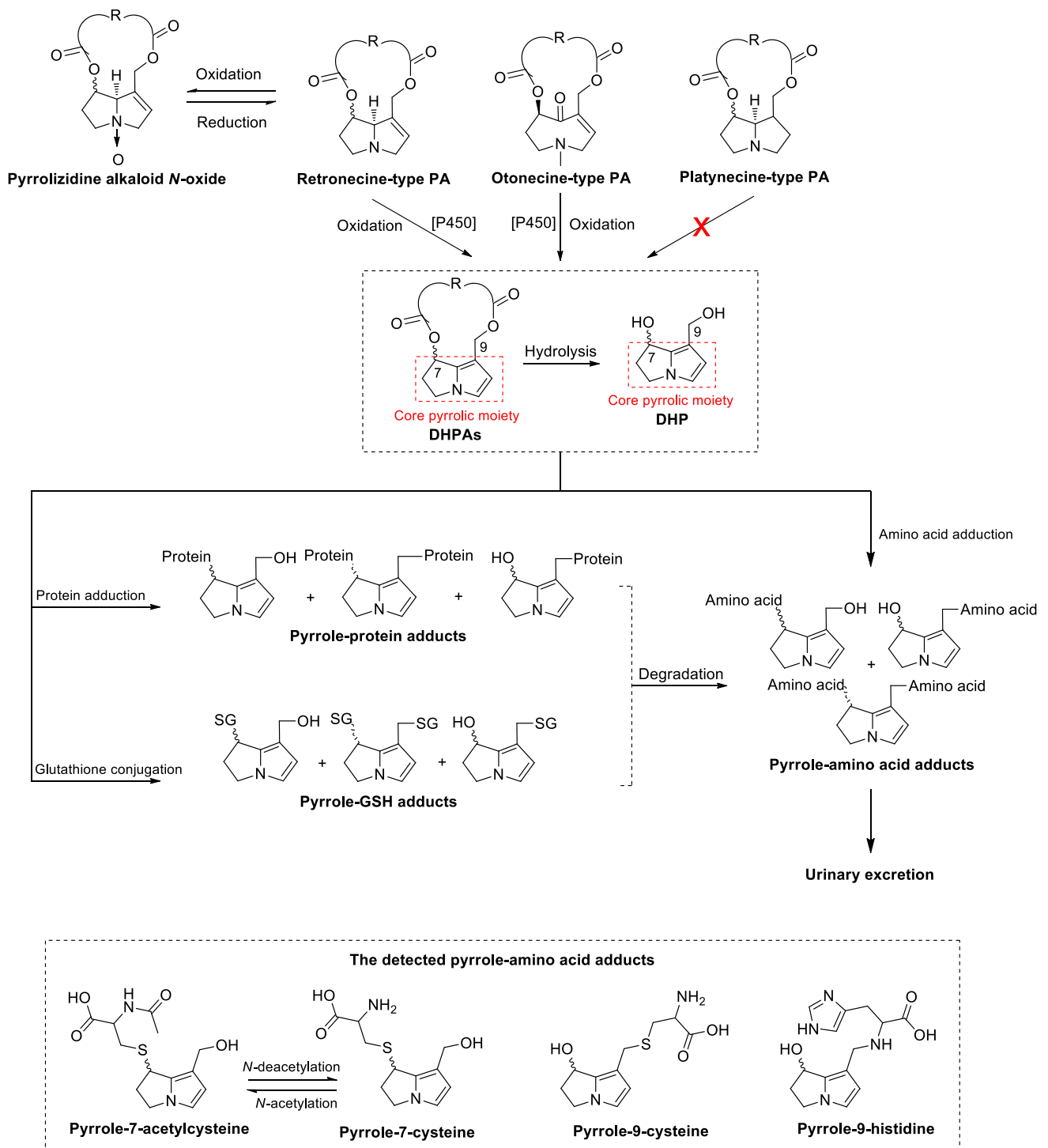


Fig. 1 A schematic illustration of metabolic activation of toxic PAs to the formation of pyrrole–protein adducts, pyrrole–GSH adducts, and pyrrole–amino acid adducts. The former two types of adducts are further degraded to pyrrole–amino acid adducts. Eventually all pyrrole–amino acid adducts are excreted from urine. The chemical structures

of four pyrrole–amino acid adducts (PAAAs) (pyrrole-7-cysteine, pyrrole-9-cysteine, pyrrole-9-histidine, and pyrrole-7-acetylcysteine) detected in RTS-treated rat and PA-ILI patient urine samples are also illustrated. DHPAs, dehydropyrrolizidine alkaloids; DHP, (\pm)-6,7-dihydro-7-hydroxy-1-hydroxymethyl-5H-pyrrolizine

Animal experiment

The care of rats and all experimental procedures were reviewed and approved by the Animal Experimental Ethics Committee of the Chinese University of Hong Kong under the regulations of the Hong Kong Special Administrative Region government. Male Sprague Dawley (SD) rats (weight 180–200 g, age 7–8 weeks) were supplied by the Laboratory Animal Service Center, the Chinese University of Hong Kong. For the single-dose study, rats ($n=5$) were orally administered with a single dose of RTS (a representative toxic PA to induce PA-ILI in rat models (Lin et al. 2011; Ruan et al. 2015; Zhu et al. 2017)) at 40 mg/kg and sacrificed on 14 days after dosing. For the multiple-dose study, rats ($n=5$) were orally administered 5 mg RTS/kg/day for 14 consecutive days and sacrificed 28 days after the last dosing. Upon sacrifice, liver tissues were removed for further analysis. For both studies, rats ($n=5$) treated in parallel with water served as controls. All treated rats were placed individually in metabolic cages and allowed free access to water and food. The 24-h (0–24 h) urine samples of individual rats were collected daily into sterilized containers kept on ice throughout the study. Collected urine samples were stored at $-80\text{ }^{\circ}\text{C}$ until PAAA analysis. The volume of individual urine samples was measured and recorded. An aliquot (200 μL) of urine sample was filtered and centrifuged at $20,000\times g$ for 15 min at $4\text{ }^{\circ}\text{C}$. The supernatant was collected, filtered, and subjected to UHPLC–MS/MS analysis.

Hematoxylin and eosin (H&E) staining

Liver samples were fixed in 4% paraformaldehyde (PFA) for 18 h at $4\text{ }^{\circ}\text{C}$ and embedded in paraffin blocks, which were further sectioned at $5\text{ }\mu\text{m}$ and stained with H&E. The sections were then examined for liver injury parameters such as central vein endothelial damage and sinusoidal dilation with a Q-imaging digital camera and Axiophot 2 upright microscope (Axioplan 2, Zeiss).

Immunohistochemical staining

The typical features of PA-induced HSOS were evaluated using our previously reported immunohistochemical staining method (Li et al. 2018; Yang et al. 2017). Rat liver samples were embedded in Tissue-Tek[®] optimum cutting temperature (O.C.T.) compound, cut into $7\text{-}\mu\text{m}$ sections, and mounted onto positively charged microslides (Super Plus slide, Menzel-Glaser). After blocking with 10% goat serum for 1 h, the liver sections were incubated with anti-endothelial cell antibody (RECA-1) (1:100 in blocking solution comprising 10% goat serum) overnight at $4\text{ }^{\circ}\text{C}$. Then, the liver sections were washed with PBS/0.2% Tween 20 (PBST) and incubated with goat anti-mouse IgG secondary antibody (Alexa

Fluor[®] 488) for 1 h at room temperature. The resultant tissue slides were stained with 4',6-diamidino-2-phenylindole (DAPI), followed by observation under a confocal system with the inverted microscope (Olympus Fluoview FV1000) with a $40\times$ objective lens.

Urine samples from PA-ILI patients

After we successfully developed the analysis of urinary PAAAs in rat models, 64 PA-ILI patients admitted to Nanjing Drum Tower Hospital, Nanjing, China, from January to October 2019, were recruited retrospectively or at admission for the urinary PAAA study after approval by the ethics committee and acquisition of informed consent. All patients claimed consumption of herb ‘Tu-San-Qi’ (*Gynura japonica*) as tonics for self-medication before the onset of liver injury with similar symptoms as those of our previously reported PA-ILI patients (Gao et al. 2012, 2015; Ruan et al. 2015). Diagnosis of PA-ILI from these DILI patients included that they: (1) met the diagnostic criteria for DILI with Roussel Uclaf Causality Assessment Method (RUCAM) score >5 (Danan et al. 2016; García-Cortés et al. 2011); (2) met the ‘Nanjing criteria’ for PA-induced HSOS (Zhuge et al. 2019); and (3) claimed a history of the intake of ‘Tu-San-Qi’, a known PA-producing herb (Ruan et al. 2015; Yang et al. 2017), for self-health improvement; however, no ingested herbal sample was provided by these patients. A total of 158 urine samples were collected at different times from 64 PA-ILI patients for the analysis of PAAAs. Among these patients, blood specimens were also collected in 43 patients and had been tested for blood PPAs in our previously reported study (Ma et al. 2020). The detailed demographics of these 64 PA-ILI patients, number of urine samples collected in individual patients, and the indication of 43 patients with their blood PPAs tested are provided in Table S1. In addition, urine samples collected from ten healthy volunteers who did not take ‘Tu-San-Qi’ or any other PA-containing products were used as controls. All collected urine samples were stored at $-80\text{ }^{\circ}\text{C}$ until PAAA analysis. An aliquot (200 μL) of each urine sample was filtered and centrifuged at $20,000\times g$ for 15 min at $4\text{ }^{\circ}\text{C}$. The supernatant was collected, filtered, and subjected to UHPLC–MS/MS analysis.

Analysis of PAAAs in urine samples by UHPLC–MS/MS

Identification and quantitation of PAAAs were performed on an Agilent 6460 Triple Quadrupole UHPLC–MS/MS System using a Waters Acquity BEH C18 column ($2.1\times 100\text{ mm}$, $1.7\text{ }\mu\text{m}$). A binary LC gradient was applied to the analytical column to separate PAAAs from the urine sample. Mobile phase A was 0.1% formic acid in water and mobile phase B

was 0.1% formic acid in acetonitrile, which were employed in the LC gradient elution method as follows: 2% B at 0–0.5 min; 2–15% B at 0.5–20 min; 15–18% B at 20–22 min; 18% B at 22–23 min; 18–60% B at 23–24 min; and 60% B at 24–27 min. The flow rate was 0.3 mL/min, the column temperature was maintained at 45 °C, and the injection volume was 2 µL.

The mass spectrometer was operated using multiple reaction monitoring (MRM) in positive-ion mode with an electrospray ionization (ESI) interface. The mass spectrometer parameters used are as follows: gas temperature was 320 °C; gas flow was 7 L/min; nebulizer gas at 45 psi; and capillary voltage was 4000 V. The MRM used for 4 PAAAs was designed based on our previous findings (He et al. 2016a, 2016b; Ma et al. 2019; Zhao et al. 2011, 2012). According to their MS/MS spectrums (Figure S1), both pyrrole-7-cysteine and pyrrole-9-cysteine were monitored at the $[M + H - H_2O]^+$ m/z 239 to $[M + H - 119]^+$ m/z 120 ion transition, pyrrole-9-histidine was monitored at the $[M + H]^+$ m/z 291 to $[M + H - 155]^+$ m/z 136 ion transition, and pyrrole-7-acetylcysteine was monitored at the $[M + H - H_2O]^+$ m/z 281 to $[M + H - 163]^+$ m/z 118 ion transition. An Agilent Mass Hunter Workstation (B.06.00) was used for UHPLC–MS/MS system operation, data acquisition, and processing.

Analytical method validation

Method validation was performed based on bioanalytical method validation guidelines for the industry published by the United State of American (USA) Food and Drug Administration (Center for Drug Evaluation and Research, USA Food and Drug Administration 2018). Selectivity of the method was tested by analyzing PAAA-free urine samples from 6 untreated SD rats and 10 healthy human volunteers. Each sample was analyzed for the exclusion of any endogenous co-eluting interferences within the peak regions of the investigated PAAA. Calibration curves were constructed by plotting the peak area *versus* the concentration of each PAAA standard dissolved in distilled water. The limit of detection (LOD) and limit of quantitation (LOQ) were determined at a signal-to-noise (S/N) ratio of about 3 and 10, respectively. The intra- and inter-day precisions were assessed by analyzing three concentrations of standards within 1 day or for 3 consecutive days, respectively. Precision was calculated and expressed in terms of % relative standard deviation (RSD, %). The matrix effect was evaluated at three concentrations, in triplicate, by comparing the peak area of individual PAAA standards spiked in blank urine with that spiked in distilled water in triplicate. Method stability, including freeze–thaw stability, autosampler stability at 4 °C, and long-term stability at – 80 °C, was evaluated in triplicate.

Data analysis

Urine kinetic parameters for both single-dose and multiple-dose studies in rats were obtained using WinNonlin (Pharsight Corporation, Mountain View, CA, USA, version 4.0). The elimination half-life ($t_{1/2}$) value was calculated based on the semi-logarithmic daily excretion rate ($\Delta Xu/\Delta t$) *versus* the mid-point of collection time interval profile. $\Delta Xu/\Delta t$ was calculated by multiplying urinary PAAA concentrations by the volume of corresponding 0–24 urine samples. Data are expressed as mean \pm standard deviation (SD) for the results of method validation and demographics and mean \pm standard error of mean (SEM) for all other measurements. All data analyses were performed by GraphPad Prism 6.0 (GraphPad Software Inc, San Diego, CA).

Results

Detection of PAAAs in urine

Four PAAAs, pyrrole-7-cysteine, pyrrole-9-cysteine, pyrrole-9-histidine, and pyrrole-7-acetylcysteine, were identified and quantified in the urine of RTS-treated rats and PA-ILI patients by UHPLC–MS/MS (Figure S2). The fully validated quantitative method with determined regression equations, linearity ranges, and correlation coefficients is summarized in Table S2. Correlation coefficient values (r^2) for the linearity of all calibration curves of 4 PAAAs were all higher than 0.993, indicating appropriate correlations within the test ranges. For all PAAAs, LOD and LOQ values were in the ranges of 0.16–0.81 nM and 0.54–2.70 nM, and overall intra- and inter-day variations (RSD%) were in the range of 1.34–3.79% and 1.94–5.36%, respectively. The matrix did not significantly affect analyses of all PAAAs with acceptable variation ranges for both rat (88.93–102.81%) and human (88.16–104.86%) urine samples (Table S3) under detection conditions. The stability of the 4 PAAAs was assessed under different preparation conditions. The results demonstrated that all 4 PAAAs were highly stable with variations within 9.47% (Table S4).

PAAAs in urine of single-dose RTS-treated rats

Based on our previous studies on RTS-induced liver injury rat models (Lin et al. 2011; Ruan et al. 2015; Zhu et al. 2017), a single dose of 40 mg RTS/kg was used to induce hepatotoxicity in rats. H&E and immunohistochemical staining results showed that RTS induced apparent hepatic sinusoidal dilation and endothelial cell damage around the central veins, which are typical features of HSOS (Fig. 2A and B). Four PAAAs were detected in the urine of all RTS-treated rats (Fig. 3A) but not in the urine of control

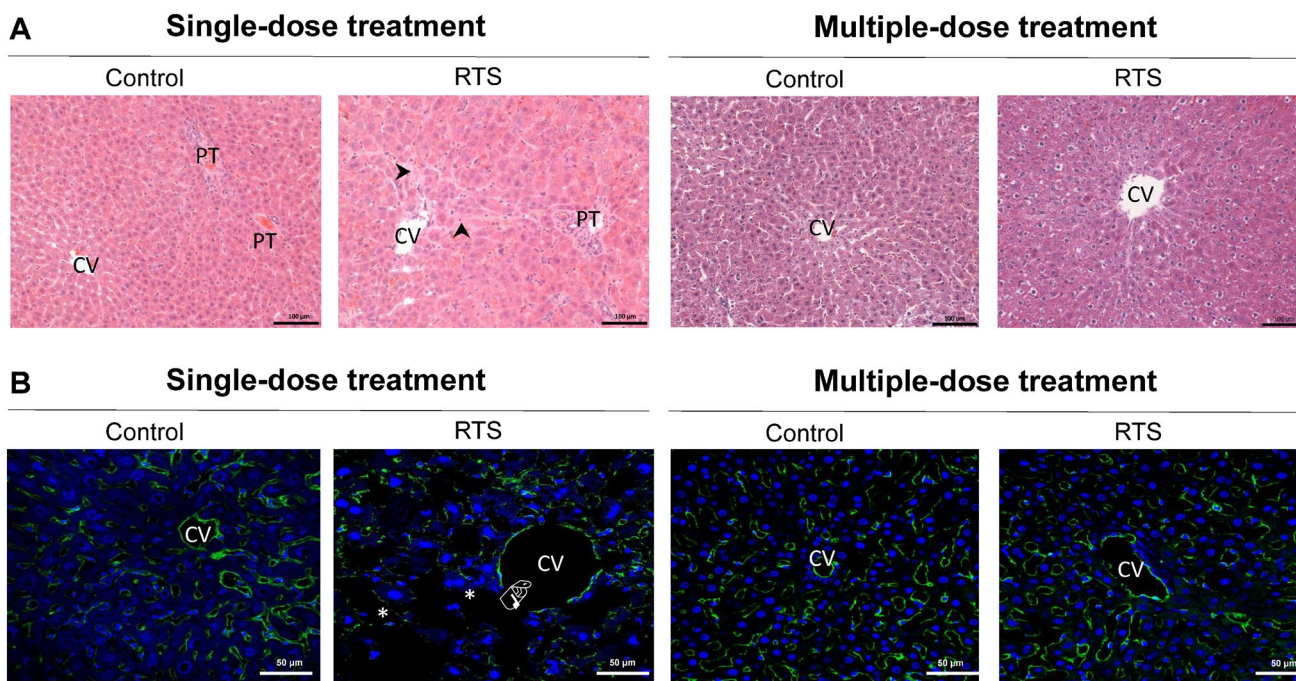


Fig. 2 Histological observation of rat liver injury. **A** Representative H&E-stained liver sections show sinusoidal dilation () in RTS-treated rats (200×magnification; scale bar 100 μm). PT designates portal vein. CV designates central vein. **B** The representative immunohistochemical staining on sinusoidal endothelial cells using RECA-1 in

green and nuclei using DAPI in blue of rat liver Sects. (400×magnification; scale bar 50 μm). indicates that endothelial cells are partly detached from lumen surface of CV. * indicates that injured sinusoids have a larger space with wider gaps among individual sinusoids

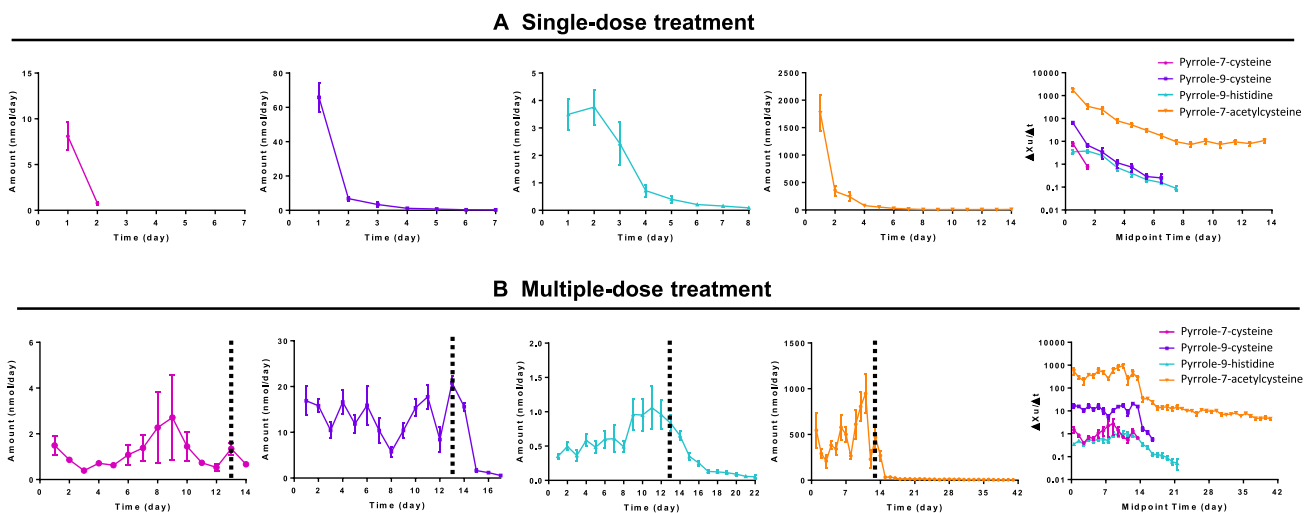


Fig. 3 Urinary excretion amount-time profiles of pyrrole-7-cysteine, pyrrole-9-cysteine, pyrrole-9-histidine and pyrrole-7-acetylcysteine of **A** rats ($n=5$) orally administered with 40 mg/kg of RTS and **B** rats ($n=5$) orally administered with 5 mg/kg/day of RTS for 14 consecu-

tive days. The semi-logarithmic daily excretion rate ($\Delta X_u/\Delta t$) versus the mid-point of collection time interval profiles for individual PAAAs

rats (Figure S2). Considering daily excretion, pyrrole-7-acetylcysteine was excreted in the greatest amount, and pyrrole-9-cysteine was excreted in a significantly greater amount than that of the other 2 PAAAs for all detectable days (Fig. 3A). About 90% of total pyrrole-7-cysteine and

pyrrole-9-cysteine excretions occurred within 24 h, while pyrrole-9-histidine and pyrrole-7-acetylcysteine excretion showed a slower elimination with most excretion occurring within 1–4 days followed by a slower phase of final elimination (Fig. 3A). Except for pyrrole-7-cysteine, which was

only detected within 2 days after dosing, the persistence of the other 3 PAAAs was much longer and was estimated to be about 4, 6, and 50 days for pyrrole-9-cysteine, pyrrole-9-histidine and pyrrole-7-acetylcysteine, respectively (Table 1). The above results demonstrated that these 4 urinary PAAAs could be unambiguously identified in the single-dose rat model with obvious PA-induced hepatotoxicity.

PAAAs in urine of multiple-dose RTS-treated rats

For the multiple-dose study, 5 mg RTS/kg/day for 14 consecutive days was used to establish the rat model with low dose but prolonged exposure to PA, which is common in human PA-poisoning cases especially induced by PA-contaminated foodstuffs. All the treated rats were sacrificed at 28 days after the last dosing. Throughout the entire study, no animal death or any obvious adverse effects, such as significant body weight loss, were observed in the rats, indicating that no obvious severe toxicity occurred. H&E and immunohistochemical staining results did not show apparent hepatic morphological changes and sinusoidal damage (Fig. 2A and B), indicating that a 14-day low dose of RTS exposure did not yet induce obvious liver injury. The 4 PAAAs which were found in the single-dose RTS-treated rats were also detected in the urine samples of all multiple-dose RTS-treated rats but not in control rat urine. During the 14-day treatment period, the daily excretion of all PAAAs fluctuated within different ranges over the time (Fig. 3B). Similar to the single-dose treated rats, the daily excreted amount of pyrrole-7-acetylcysteine was the greatest with at least 100 times more than that of

the other 3 PAAAs, and the amount of pyrrole-9-cysteine was significantly higher than that of pyrrole-7-cysteine and pyrrole-9-histidine in all days of the treatment period. After the withdrawal of RTS, pyrrole-7-cysteine and pyrrole-9-cysteine could not be detected on day 2 and day 5 after the last dosing, respectively, while prolonged urinary excretion of pyrrole-9-histidine and pyrrole-7-acetylcysteine were observed (Fig. 3B). The estimated persistence of pyrrole-7-acetylcysteine, pyrrole-9-histidine, and pyrrole-9-cysteine were similar to those determined in the single-dose model (Table 1). While, for pyrrole-7-acetylcysteine, after the last RTS exposure, the elimination kinetic showed nearly half of the total amount was rapidly excreted within 2 days; the remainder was then eliminated at a significantly slower rate and was still detectable on the last experimental day, i.e. 28 days after RTS withdrawal (Fig. 3B) with an estimated persistent time of 60 days (Table 1). The results demonstrated that these 4 PAAAs could also be detected in the low but prolonged PA exposure rat model with no obvious hepatotoxicity.

Based on the findings from both single- and multiple-dose rat models, the superiority of 4 PAAAs was ranked as: pyrrole-7-acetylcysteine >>> pyrrole-9-histidine \approx pyrrole-9-cysteine >>> pyrrole-7-cysteine. Furthermore, the results indicated that daily amounts of urinary excretion of these urinary PAAAs varied significantly along with sampling time within the same animal and were not clearly related to the severity of PA-ILI. Therefore, the determination of these urinary PAAAs could serve as a specific and reliable test for PA exposure regardless of the exposed dosage regimen and the severity of the injury.

Table 1 Kinetic parameters of urinary PAAAs in RTS-treated rats

PAAA	Single dose (RTS, <i>p.o.</i> , 40 mg/kg)				Multiple dose (RTS, <i>p.o.</i> , 5 mg/kg/day for 14 consecutive days)			
	$t_{1/2}^a$ (day)	Persistent time (day)		Total excretion (nmol) (% dosed PA)	$t_{1/2}^a$ (day)	Persistent time (day)		Total excretion (nmol) (% dosed PA)
		Observed	Calculated ^b			Observed	Calculated ^b	
Pyrrole-7-cysteine	N.A	2	N.A	8.87 ± 1.67 (0.04%)	N.A	1	N.A	15.29 ± 2.79 (0.04%)
Pyrrole-9-cysteine	0.76 ± 0.05	7	3.8	78.53 ± 10.55 (0.34%)	0.68 ± 0.03	4	3.4	195.34 ± 16.52 (0.49%)
Pyrrole-9-histidine	1.19 ± 0.07	8	6.0	11.26 ± 2.08 (0.05%)	1.99 ± 0.16	9	10.0	10.56 ± 1.63 (0.03%)
Pyrrole-7-acetylcysteine	10.10 ± 0.43	14 ^c	50.5	2594.73 ± 408.03 (11.38%)	12.12 ± 1.39	28 ^c	60.6	6761.87 ± 572.90 (16.99%)

^aThe elimination half-life ($t_{1/2}$) was calculated based on the terminal phase of post-dosing period

^bThe calculated persistent time (the time after the last dosing) was estimated as five times of $t_{1/2}$

^cPyrrole-7-acetylcysteine was still detectable on the sacrificed day (at 14 and 28 days after withdrawal of RTS in both single- and multiple-dose studies)

N.A.: not applicable

Determination of PAAAs in urine of PA-ILI patients

Urine samples were tested from 64 PA-ILI patients (39 males and 25 females) with the median age of 65 years old ranging from 43 to 80. Demographic and clinical features of these patients are shown in (Fig. 4A). The patients all claimed the consumption of a PA-containing herb *G. japonica*, with decoction as the most common form. The onset of liver injury mainly occurred after the intake of *G. japonica* from 3 days to 5 years. Their RUCAM scores were 6.7% at 5, 60.0% at 6–8, and 33.3% at 9–10, indicating a high possibility of DILI. About 50% of patients presented as cholestatic injury, ~26% as hepatocellular injury and ~23% as mixed injury. Only a part of patients manifested typical symptoms of PA-induced HSOS, such as ascites (61/64), jaundice (36/64), and hepatomegaly (31/64), presenting a diagnostic challenge to the clinicians. Besides, most patients showed no or mildly elevated levels of conventional serological markers (ALT, AST, and total bilirubin) in routine liver function tests, further increasing the difficulties for clinical diagnosis and identification of the etiology. Furthermore, computed tomography (CT) scans were performed in limited numbers of patients, and the representative CT scan images of two patients indicated apparent pathological changes, such as

hepatomegaly, patchy enhancement in the liver, and ascites, etc. (Fig. 4B, C), but cannot clearly differentiate damage severities among the patients or distinguish from other types of liver diseases.

A total of 158 urine specimens were collected from 64 PA-ILI patients at different times (Table S1). Among them, 53 patients provided urine samples upon their admission to the hospital, while 11 patients were retrospectively recruited after discharge from hospital and could not provide urine samples upon admission. Among these 11 patients, 6 patients provided only one urine sample at 6 ($n=4$) or 10 ($n=2$) months after admission. Due to the manner of recruiting patients into the study, the sampling time and number of urine samples collected from individual patients could not be as well-controlled as in a conventional well-designed cohort study. The numbers of samples from each patient collected over scattered sampling times were: 1 sample (21 patients), 2 samples (15 patients), 3 samples (12 patients), 4 samples (10 patients), 5 samples (5 patients), and 6 samples (1 patient). Detailed information on the number of urine samples from individual patients is provided in Table S1.

About 82% samples collected from ~91% of the patients showed at least one detectable PAAA (Fig. 5), while no PAAAs were detected in urine from any healthy subject. For

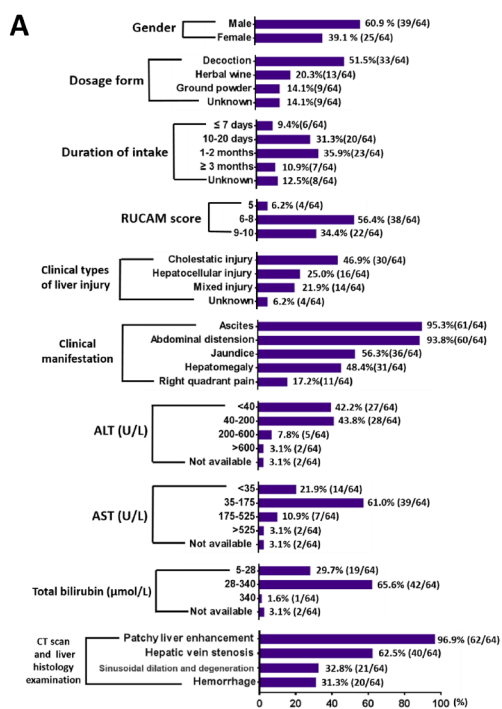
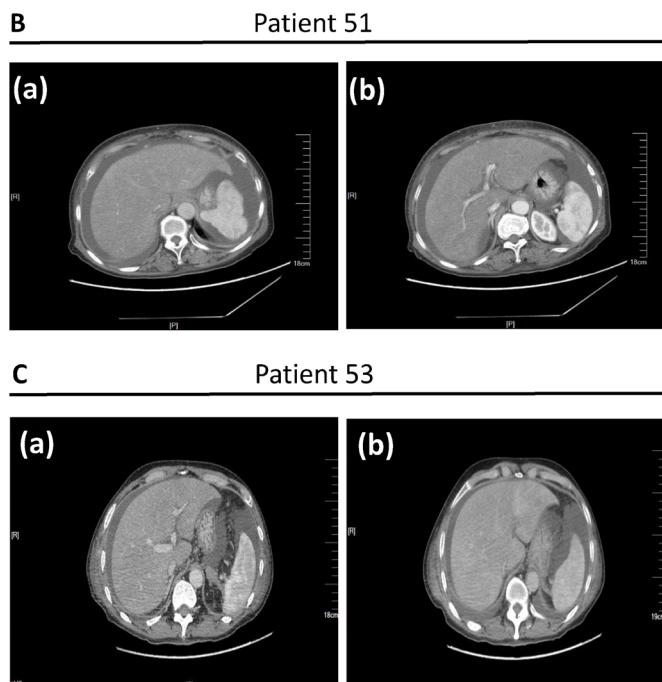


Fig. 4 Demographic and clinical features of 64 PA-ILI patients (A). Representative CT scan imaging of patient 51 (B) shows (a) hepatomegaly, mottle-like heterogeneous enhancement in the arterial phase, thickening of hepatic artery branches, and ascites; (b) heterogeneous, patchy decreased density of the hepatic parenchyma and ascites. Representative CT scan imaging of patient 53 (C) shows (a) hepatomegaly,



ally, diffuse patchy hepatic enhancement; (b) heterogeneous, patchy decreased density of the hepatic parenchyma and ascites. RUCAM, Roussel Uclaf Causality Assessment Method; ALT normal reference range: <40 U/L; AST normal reference range: <35 U/L; total bilirubin normal reference range: 5–28 μmol/L (Zhu et al. 2020)

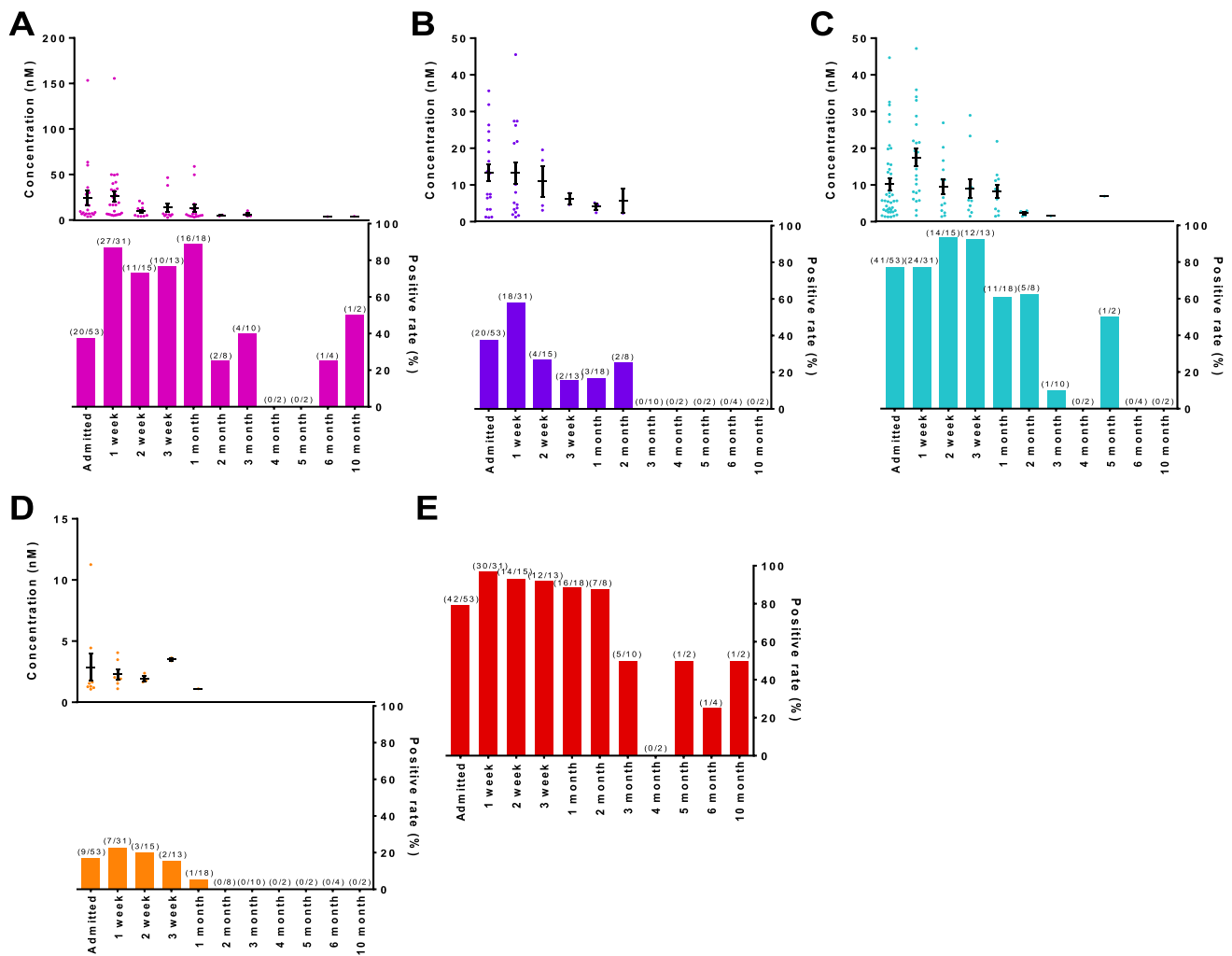


Fig. 5 Concentration and positive rate of pyrrole-7-cysteine (A), pyrrole-9-cysteine (B), pyrrole-9-histidine (C), and pyrrole-7-acetylcysteine (D), and positive rate of all 4 PAAAs (E) determined in 158 urine samples from 64 PA-ILI patients

the quantitation, different from the animal study, PAAA urinary concentrations rather than total daily excreted amounts were measured, because small volumes of urine sample rather than a total 24-h urine sample were collected. The number of PAAAs and their urinary concentrations in individual patients varied significantly, while in general urinary levels of all 4 PAAAs gradually decreased with time (Fig. 5). Due to the nature of this non-cohort toxicological study with scattered sampling times from individual patients, we selected ten urine samples collected at 3 months after hospital admission, which could be considered as the longest sampling time with adequate samples, to further estimate the persistence of individual PAAAs. Results indicated that pyrrole-7-cysteine (Fig. 5A) and pyrrole-9-histidine (Fig. 5C) were detected in 40% and 10% of all 3-month urine samples, while both pyrrole-9-cysteine (Fig. 5B) and pyrrole-7-acetylcysteine (Fig. 5D) were not detected in any 3-month urine samples. In addition, pyrrole-7-cysteine was detected in 1/4

of 6-month and 1/2 of 10-month urine samples (Fig. 5A), while pyrrole-9-histidine was detected in 1/2 of 5-month urine samples (Fig. 5C), indicating both pyrrole-7-cysteine and pyrrole-9-histidine showed significantly longer persistence. However, the numbers ($n = 8$) of samples collected at 5 months or beyond were limited and were the only sample provided by each of eight patients who were admitted to and discharged from the hospital prior to the start of the present study. These patients were recruited and sampled only when they re-visited the hospital after discharge. Further tests of more samples repeatedly collected from individual patients over comparable periods are warranted to confirm such long persistence of these two PAAAs.

Furthermore, about 2–5 urine samples were repeatedly collected upon admission until 1 month after admission in ten patients. Similar to the results of rat studies, both presence and concentration of urinary 4 PAAAs varied remarkably at different times. For instances, in the samples

collected upon or 1 month after admission, the PAAA-positive rate was 20% or 10% for all 4 PAAAs; 40% or 10% for 3 PAAAs; 10% or 60% for 2 PAAAs, and 20% or 10% for 1 PAAA (Fig. 6A). With the sample availability, 4 of these patients were selected for further investigation of urinary PAAA excretion kinetic profiles in 4–5 urine samples. In general, less numbers of PAAAs were detected along with time and urinary concentrations of pyrrole-7-acetylcysteine were significantly lower than that of other 3 PAAAs at all sampling times in all four patients (Fig. 6B). For individual PAAAs, scattered urine concentrations were observed along with time, which were mainly affected by the varied volume and frequency of bladder emptying, and different excretion kinetics of individual PAAAs.

Considering all results, especially the maximum and median concentrations determined in urine collected within 3 months after admission (Table 2), the order for the determination of 4 PAAAs in humans appeared to be pyrrole-7-cysteine > pyrrole-9-histidine ≈

pyrrole-9-cysteine >>> pyrrole-7-acetylcysteine. Apparently, the detection rank order of 4 PAAAs was different in human and rats and the reasons for such difference are explained in the following discussion session. Nevertheless, based on the findings in human, we suggested that the combined application of all 4 PAAAs with the detection of at least one of them could be regarded as PAAA-positive, and such combined PAAA application could remarkably improve positive detection (Fig. 5E).

In addition, the clinic features of the aforementioned 4 representative patients were also compared and found without specific differences in symptoms of liver injury with no or mildly elevated ALT, AST, and total bilirubin levels measured upon admission (Table 3). Although the results of liver CT scans or histological examination indicated apparent pathological changes, the severity varied among individuals and was indistinguishable from possible diagnoses from other insults, such as BCS, decompensated cirrhosis, infection, alcoholic, or other drugs. Furthermore, similar

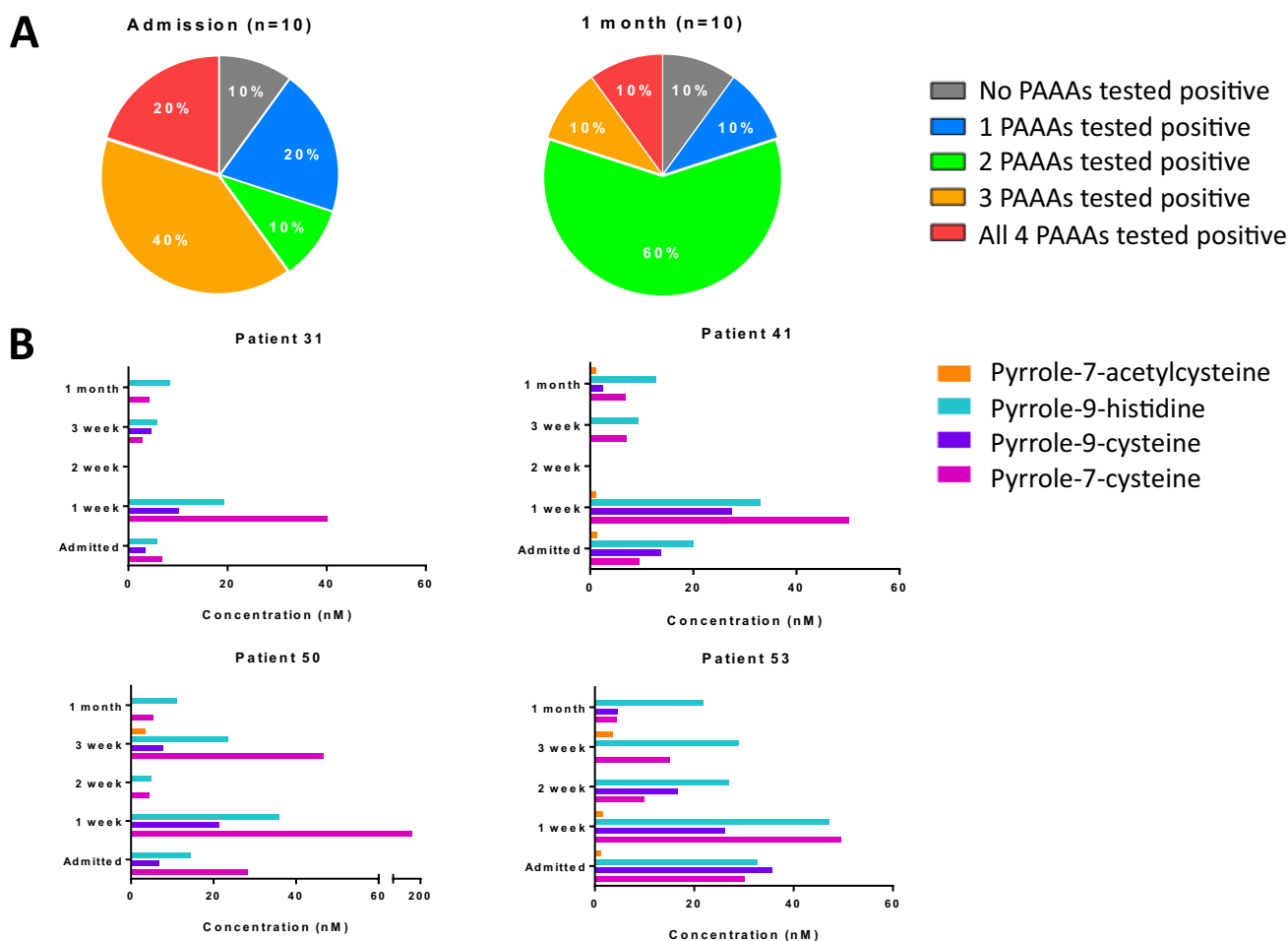


Fig. 6 The percentage of individual PAAAs detected in urine samples from ten patients collected upon hospital admission and 1 month after admission (**A**), and the concentration of individual PAAAs deter-

mined in urine samples from 4 patients collected at 4 (Patient 31 and Patient 41) or 5 (Patient 50 and Patient 53) different times (**B**)

Table 2 Concentration of individual PAAAs determined in PA-ILI patients' urine samples collected within 3 months after admission to hospital

Sampling time	Median concentration (concentration range) (nM)			
	Pyrrole-7-cysteine	Pyrrole-9-cysteine	Pyrrole-9-histidine	Pyrrole-7-acetylcysteine
Admission	8.97 (3.78–153.37)	12.29 (1.16–35.63)	5.70 (1.33–44.67)	1.55 (1.07–11.25)
1 week	16.78 (4.91–155.66)	9.07 (1.29–45.54)	15.61 (1.70–47.18)	1.92 (1.11–4.05)
2 weeks	8.24 (4.07–20.94)	10.55 (3.09–19.55)	7.18 (1.41–26.92)	1.75 (1.66–2.38)
3 weeks	6.09 (2.83–46.55)	6.18 (4.63–7.72)	6.18 (1.48–28.99)	3.51 (3.38–3.63)
1 month	5.73 (3.03–58.84)	4.63 (2.45–5.15)	8.43 (1.48–21.89)	1.11 ^a
2 months	4.97 (4.40–5.53)	5.60 (2.32–8.88)	2.52 (1.48–2.96)	N.D
3 months	5.22 (4.29–10.24)	N.D	1.56 ^a	N.D

N.D.: not detected

^aPAAA was only detected in one sample**Table 3** The clinic characteristics of four representative patients

Patient code	P31	P41	P50	P53
RUCAM score	9	7	8	9
Clinical manifestation				
Jaundice	√	√	√	×
Ascites	√	√	√	√
Hepatomegaly	√	√	×	×
ALT (U/L) (NRR: < 40 U/L)	118.8	177	120.4	198.4
AST (U/L) (NRR: < 35 U/L)	69.9	107	89.5	259.3
Total bilirubin (μmol/L) (NRR: 5–28 μmol/L)	22.3	26.2	64	77.5
CT scan or liver histological examination				
Patchy liver enhancement	√	√	√	√
Hepatic vein stenosis	√	×	√	×
Hepatic sinusoidal dilation and degeneration	√	×	×	×
Hemorrhage	√	×	×	×

NRR: normal reference range (Zhu et al. 2020)

to the results obtained from rat models, the findings also revealed no obvious correlation between urinary PAAAs levels and clinical characteristics (such as serum ALT and AST levels) measured upon admission of 53 PA-ILI patients (Figure S3). On the other hand, the findings from urinary test revealed the unequivocal presence of 4 PAAAs in urines collected at different times from all patients, which provide reliable evidence for PA exposure, and thus could be used as a specific test to diagnose PA-ILI in the clinic.

Discussion

In the present study, we reported the development of a non-invasive approach for the identification of PA-ILI in the clinic. We first identified and quantified 4 PAAAs, pyrrole-7-acetylcysteine, pyrrole-9-histidine, pyrrole-9-cysteine, and

pyrrole-7-cysteine, in the urine of rats treated with RTS in both single- and multiple-dose models. Orders for the excretion amounts of PAAAs were found similar in both models with pyrrole-7-acetylcysteine being predominant. We further confirmed that these 4 PAAAs were also excreted in the urine of PA-ILI patients with at least 1 PAAA detected in ~91% patients (Fig. 5), while no PAAAs were detected from urine of healthy people. This developed clinical approach for testing PAAAs in the urine of PA-ILI patients requires a low sample volume (200 μl urine), minimal sample handling and fast sample processing (within 30 min), and moderate instrument time (27 min in LC gradient), providing the first non-invasive diagnosis of PA exposure in patients.

Currently, the causes of formation for these PAAAs are largely unclear. To date, only pyrrole-7-acetylcysteine has been detected in the urine of male SD rats administered ¹⁴C-monocrotaline or ¹⁴C-senecionine (Estep et al. 1990). Moreover, pyrrole-7-cysteine was identified from human and rat liver microsomal metabolism of riddelliine via CYPs-mediated formation of DHPA followed by interaction with cysteine (He et al. 2016b). Limited available information suggests that urinary PAAAs can not only be degraded from PPAAs bound with blood proteins and other proteins in various organs/tissues, but also from the direct binding of DHPAs with GSH and amino acids in the body (Fig. 1), which therefore can result in higher concentrations and longer persistence than that of PPAAs in blood. The formation of xenobiotic-derived GSH adducts followed by sequential enzymes-mediated degradations to generate cysteinylglycine adducts, cysteine adducts and acetylcysteine adducts, are called mercapturic degradation pathway, which is generally considered as a detoxication pathway for xenobiotics. The resultant degraded adducts, especially cysteine adducts and acetylcysteine adducts, which are called mercapturic acids via *N*-acetylation of cysteine adducts, are polar and readily excreted from urine (Hanna et al. 2019). Nevertheless, the detailed mechanisms underlying the PAAAs formation via

breakdown from different pyrrole proteins and urinary elimination are largely unknown and warrant future investigation.

In patient urine, pyrrole-7-cysteine was predominant with the longest persistence and pyrrole-7-acetylcysteine showed the lowest concentrations with the shortest persistence, while opposite observations were found in PA-treated rats. Because these 2 PAAAs are interconverted via *N*-acetylation and *N*-deacetylation in the body (Fig. 1), there are three plausible explanations for the observed species difference. First, rats have been reported to have a significantly higher *S*-conjugate *N*-acetyltransferase activity than humans (Chasseaud 1976; Green et al. 2003; Heuner et al. 1991). Second, aminoacylases, which hydrolyze acetylated cysteine *S*-adducts back to cysteine *S*-adducts via *N*-deacetylation, are defective in rat species (Anders et al. 1994; Hanna et al. 2019). Third, the rate of *N*-deacetylation was greater than that of *N*-acetylation in humans (Altuntas et al. 2002). Therefore, with lower *N*-acetylation of cysteine *S*-adduct but higher *N*-deacetylation of acetylated cysteine *S*-adducts, pyrrole-7-cysteine was excreted as a predominant form, while pyrrole-7-acetylcysteine was excreted as a minor form in the urine of PA-ILI patients. However, for a confirmative comparison, both sexes of different species should be involved, while only male rat was investigated in the present study; therefore, a more comprehensive investigation with both sexes of rat and human is warranted in the future study.

Apart from the significant differences in urinary excretion and persistence of pyrrole-7-cysteine and pyrrole-7-acetylcysteine between PA-ILI patients and PA-treated rats, quantitative measurements of 4 PAAAs were also different between human and rat urine samples. While daily excreted amounts of individual PAAAs were determined from the total urine excreted from rats, more practical for the clinical test, only small volume of urine was collected from patients, and thus, concentration rather than total daily amount of individual PAAAs in urine was determined. However, concentrations of individual PAAAs in the urine continuously change with time due to variations of urine volume and frequency of bladder emptying. Therefore, unavoidably, the selection of a particular PAAA as the test for PA exposure may lead to a false-negative result, while the simultaneous determination of 4 PAAAs would undoubtedly assist the confirmative identification of PA exposure. Apparently because of the aforementioned species difference, the study of kinetics of urinary elimination of PAAAs in PA-ILI patients is significantly challenging and cannot be predicted from the data determined from PA-treated rats. Nevertheless, further investigations on human urinary elimination kinetics of PAAAs are certainly warranted.

The results obtained from both PA-treated rats and PA-ILI patients demonstrated that either total amounts or concentrations of PAAAs in urine could not be directly correlated to the severity of PA-ILI. Besides, the levels of urinary PAAAs

may also vary due to other factors, including (a) amount and type of PAs consumed, (b) duration of consumption, and (c) time of specimen sampling. These information are usually lacking or cannot be provided accurately in most clinical poisoning cases, because it is not a general practice to properly record such information by consumers who expose to PA-containing products for self-medication, self-health-improvement, or accidental consumption of PA-containing products and/or PA-contaminated foodstuffs. Therefore, similar to the viral RNA fragment test for the diagnosis of coronavirus disease 2019 to confirm that the subject is infected by coronavirus 2 but unrelated to the severity of the infectious, the detection of PAAAs can only provide the positive result for PA exposure, but not directly reflect the severity of liver injury.

The value of any biomonitoring approach depends upon its ability to accurately classify individuals with disparate exposures and, ultimately, the risk of disease. Therefore, the method described here was used to discriminate between individuals with disparate exposures of PAs.

Currently, there is no officially approved biomarker/test to definitively identify PA exposure as the cause of liver injury in patients. On the other hand, our previously developed blood PPA test, in particular serum/plasma pyrrole–plasma protein adducts (PPPAs) test, has been applied for clinic test to confirm PA exposure and confirmative diagnosis of PA-ILI in many liver injury patients in China (Lin et al. 2011; Ruan et al. 2015; Yang et al. 2017) and Ethiopia (The USA Centers for Disease Control and Prevention (CDC) 2012), and has also been recommended by The Hepatobiliary Diseases Committee of Chinese Society of Gastroenterology to include blood PPPA test as one of the diagnostic criteria for PA-induced HSOS, in case patients cannot provide the history or only provide an ambiguous history of the intake of drug/herb (Zhuge et al. 2019). Recently, we further developed a pyrrole–hemoglobin adducts (PHAs) test in red blood cells (Ma et al. 2019) and revealed that PHAs had significantly higher level and longer persistence than that of PPPAs (Ma et al. 2020). In the present 64 PA-ILI patients with urinary PAAA test, 43 patients have been previously tested for both PPPAs and PHAs (Table S1) (Ma et al. 2020). Comparing the results among blood PPPA and PHA tests, and urinary PAAA test in 43 patients, although the number of specimens collected and the sampling times for blood and urine samples were different in many patients, PAAA-positive results were obtained in all PHAs positive patients, while about 79% (34/43) patients were PPPAs positive (Ma et al. 2020). With the limited number of samples collected at different sampling times, the persistence of urine PAAAs appeared to be longer than that of blood PHAs; however, further investigation with adequate number and time for both biological specimens are required to confirm this finding. Taken together, the urinary PAAAs test has the advantages

of a non-invasive approach, simple sample preparation process, direct analysis, and potentially longer persistence over the currently available PA exposure biomarkers, namely blood PPPAs and PHAs.

In conclusion, a novel and non-invasive test of four urinary PAAAs has been developed for a specific determination of PA exposure in PA-ILI patients. We propose PAAAs as the non-invasive biomarker of PA exposure, and the measurement of all 4 PAAAs with the consideration of at least one detectable PAAA in the urine as the unequivocal identification of PA exposure in suspected patients for assisting the definitive diagnosis of PA-ILI in the clinic.

Supplementary Information The online version contains supplementary material available at <https://doi.org/10.1007/s00204-021-03129-6>.

Funding The present study was supported by Research Grant Council of Hong Kong SAR (GRF Grant No. 14106318) and CUHK Direct Grant (Grant No: 4054503). This article is not an official USA Food and Drug Administration (FDA) guidance or policy statement. No official support or endorsement by the USA FDA is intended or should be inferred.

Declarations

Conflict of interest Ge Lin, Lin Zhu, Jiang Ma, Chunyuan Zhang, and Yisheng He have a patent (USA Provisional Patent No.: 62/987,769) related to this work. Other authors have declared no potential conflicts of interest.

References

- Altuntas TG, Kharasch ED (2002) Biotransformation of L-cysteine S-conjugates and N-acetyl-L-cysteine S-conjugates of the sevoflurane degradation product fluoromethyl-2,2-difluoro-1-(trifluoromethyl)vinyl ether (compound A) in human kidney in vitro: interindividual variability in N-acetylation, N-deacetylation, and b-lyase-catalyzed metabolism. *Drug Metab Dispos* 30(2):148–154
- Anders MW, Dekant W (1994) Aminoacylases. *Adv Pharmacol* 27:433–448
- Center for Drug Evaluation and Research, USA Food and Drug Administration. (2018). Bioanalytical Method Validation Guidance for Industry. <https://www.fda.gov/regulatory-information/search-fda-guidance-documents/bioanalytical-method-validation-guidance-industry>
- Cao Y, Colegate SM, Edgar JA (2008) Safety assessment of food and herbal products containing hepatotoxic pyrrolizidine alkaloids: interlaboratory consistency and the importance of N-oxide determination. *Phytochem Anal* 19(6):526–533
- Chasseaud LF (1976) Conjugation with glutathione and mercapturic acid excretion. In: Arias IM, Jakoby W (eds) *Glutathione: metabolism and function*. Raven Press, New York, pp 77–114
- Chojkier M (2003) Hepatic sinusoidal-obstruction syndrome: toxicity of pyrrolizidine alkaloids. *J Hepatol* 39(3):437–446
- Danan G, Teschke R (2016) RUCAM in drug and herb induced liver injury: the update. *Int J Mol Sci* 17(1):14
- DeLeve LD, McCuskey RS, Wang X, Hu L, McCuskey MK, Epstein RB, Kanel GC (1999) Characterization of a reproducible rat model of hepatic veno-occlusive disease. *Hepatology* 29(6):1779–1791
- Edgar JA, Molyneux RJ, Colegate SM (2015) Pyrrolizidine alkaloids: potential role in the etiology of cancers, pulmonary hypertension, congenital anomalies, and liver disease. *Chem Res Toxicol* 28(1):4–20
- Edgar JA, Smith LW. (1999). Transfer of pyrrolizidine alkaloids into eggs: food safety implications. ACS Symposium Series. Volume 745, Chapter 8:118–128.
- Estep JE, Lame MW, Jones AD, Segall HJ (1990) N-acetylcysteine-conjugated pyrrole identified in rat urine following administration of two pyrrolizidine alkaloids, monocrotaline and senecionine. *Toxicol Lett* 54(1):61–69
- Fu PP, Xia Q, Lin G, Chou MW (2004) Pyrrolizidine alkaloids—genotoxicity, metabolism enzymes, metabolic activation, and mechanisms. *Drug Metab Rev* 36(1):1–55
- Fu pp. (2017) Pyrrolizidine alkaloids: metabolic activation pathways leading to liver tumor initiation. *Chem Res Toxicol* 30(1):81–93
- Gao H, Li N, Wang J, Zhang S, Lin G (2012) Definitive diagnosis of hepatic sinusoidal obstruction syndrome induced by pyrrolizidine alkaloids. *J Dig Dis* 13(1):33–39
- Gao H, Ruan J, Chen J, Li N, Ke C, Ye Y, Lin G, Wang J (2015) Blood pyrrole-protein adducts as a diagnostic and prognostic index in pyrrolizidine alkaloid-hepatic sinusoidal obstruction syndrome. *Drug Des Dev Ther* 9:4861–4868
- García-Cortés M, Stephens C, Lucena MI, Fernández-Castañer A, Andrade RJ (2011) Causality assessment methods in drug induced liver injury: strengths and weaknesses. *J Hepatol* 55(3):683–691
- Green T, Lee R, Farrar D, Hill J (2003) Assessing the health risks following environmental exposure to hexachlorobutadiene. *Toxicol Lett* 138(1–2):63–73
- Hanna PE, Anders MW (2019) The mercapturic acid pathway. *Crit Rev Toxicol* 49(10):819–929
- He XB, Ma L, Xia QS, Fu PP (2016a) 7-N-Acetylcysteine-pyrrole conjugated-a potent DNA reactive metabolite of pyrrolizidine alkaloids. *J Food Drug Anal* 24(4):682–694
- He XB, Xia QS, Ma L, Fu PP (2016b) 7-cysteine-pyrrole conjugate: A new potential DNA reactive metabolite of pyrrolizidine alkaloids. *J Environ Sci Health, Part C Environ Carcinog Ecotoxicol Rev* 34(1):57–76
- He Y, Zhu L, Ma J, Wong L, Zhao Z, Ye Y, Fu PP, Lin G (2020) Comprehensive investigation and risk study on pyrrolizidine alkaloid contamination in Chinese retail honey. *Environ Pollut* 267:115542. <https://doi.org/10.1016/j.envpol.2020.115542>
- He Y, Lian W, Ding L, Fan X, Ma J, Zhang QY, Ding X, Lin G (2021a) Lung injury induced by pyrrolizidine alkaloids depends on metabolism by hepatic cytochrome P450s and blood transport of reactive metabolites. *Arch Toxicol* 95(1):103–116
- He Y, Shi M, Wu X, Ma J, Ng TP, Xia Q, Zhu L, Fu PP, Man K, Tsui KW, Lin G (2021b) Mutational signature analysis reveals widespread contribution of pyrrolizidine alkaloid exposure to human liver cancer. *Hepatology*. <https://doi.org/10.1002/hep.31723>
- Heuner A, Dekant W, Schwegler JS, Silbernagl S (1991) Localization and capacity of the last step of mercapturic acid biosynthesis and the reabsorption and acetylation of cysteine S-conjugates in the rat kidney. *Pflügers Archiv European J Physiol* 417(5):523–527
- Kakar F, Akbarian Z, Leslie T, Mustafa ML, Watson J, van Egmond HP, Omar MF, Mofleh J (2010) An outbreak of hepatic veno-occlusive disease in Western Afghanistan associated with exposure to wheat flour contaminated with pyrrolizidine alkaloids. *J Toxicol* 2010:7. <https://doi.org/10.1155/2010/313280>
- Kempf M, Heil S, Haßlauer I, Schmidt L, von der Ohe K, Theuring C, Reinhard A, Schreier P, Beuerle T (2010) Pyrrolizidine alkaloids in pollen and pollen products. *Mol Nutr Food Res* 54(2):292–300
- Li YH, Tai WCS, Khan I, Lu C, Lu Y, Wong WY, Chan WY, Hsiao WLW, Lin G (2018) Toxicoproteomic assessment of liver responses to acute pyrrolizidine alkaloid intoxication in rats. *J*

- Environ Sci Health, Part C Environ Carcinog Ecotoxicol Rev 36(2):65–83
- Lin G, Cui YY, Hawes EM (2000) Characterization of rat liver microsomal metabolites of clivorine, an hepatotoxic otonecine-type pyrrolizidine alkaloid. *Drug Metab Dispos* 28(12):1475–1483
- Lin G, Wang JY, Li N, Li M, Gao H, Ji Y, Zhang F, Wang H, Zhou Y, Ye Y, Xu HX, Zheng J (2011) Hepatic sinusoidal obstruction syndrome associated with consumption of *Gynura segetum*. *J Hepatol* 54(4):666–673
- Lu Y, Ma J, Song Z, Ye Y, Fu PP, Lin G (2018) The role of formation of pyrrole-ATP synthase subunit beta adduct in pyrrolizidine alkaloid-induced hepatotoxicity. *Arch Toxicol* 92(11):3403–3414
- Ma L, Zhao HQ, Xia Q, Cai L, Fu pp. (2015) Synthesis and phototoxicity of isomeric 7,9-diglutathione pyrrole adducts: Formation of reactive oxygen species and induction of lipid peroxidation. *J Food Drug Anal* 23(3):577–586
- Ma J, Ruan JQ, Chen XM, Li DP, Yao S, Fu PP, Ye Y, Gao H, Wang JY, Lin G (2019) Pyrrole-hemoglobin adducts, a more feasible potential biomarker of pyrrolizidine alkaloid exposure. *Chem Res Toxicol* 32:1027–1039
- Ma J, Zhang W, He YS et al (2020) Clinical application of pyrrole-hemoglobin adducts as a biomarker of pyrrolizidine alkaloid exposure in humans. *Arch Toxicol*. <https://doi.org/10.1007/s00204-020-02947-4>
- Mattocks AR (1982) Hydrolysis and hepatotoxicity of retronecine diesters. *Toxicology Letter* 14(1–2):111–116
- Mattocks AR (1986) Chemistry and toxicology of pyrrolizidine alkaloids. Academic Press, London
- Molyneux R, Gardner D, Colegate S, Edgar J (2011) Pyrrolizidine alkaloid toxicity in livestock: a paradigm for human poisoning? *Food Addit Contam Part A* 28(3):293–307
- Ruan J, Gao H, Li N, Xue J, Chen J, Ke C, Ye Y, Fu PP, Zheng J, Wang J, Lin G (2015) Blood pyrrole–protein adducts A biomarker of pyrrolizidine alkaloid-induced liver injury in humans. *J Environ Sci Health Part C* 33(4):404–421
- Shrenk D, Gao L, Lin G, Mahony C, Mulder P, Peijnenburg A, Pfuhrer S, Rietjens I, Rutz L, Steinhoff B, These A (2020) Pyrrolizidine alkaloids in food and phytomedicine: Occurrence, exposure, toxicity and risk assessment - A review. *Food Chem Toxicol* 136:111107. <https://doi.org/10.1016/j.fct.2019.111107>
- Song Z, He Y, Ma J, Fu PP, Lin G (2020) Pulmonary toxicity is a common phenomenon of toxic pyrrolizidine alkaloids. *J Environ Sci Health Part C Environ Carcinog Ecotoxicol Rev* 38(2):124–140
- USA Centers for Disease Control and Prevention (CDC). (2012). Investigating liver disease in Ethiopia. [updated 2012 Oct 30; cited 2020 Sep 02]. Available from: <https://www.cdc.gov/nceh/stories/ethiopia.html>
- Williams MT, Warnock BJ, Betz JM, Beck JJ, Gardner DR, Lee ST, Molyneux RJ, Colegate SM (2011) Detection of high levels of pyrrolizidine-N-oxides in the endangered plant *Cryptantha crasipes* (Terlingua Creek Cat's-eye) using HPLC-ESI-MS. *Phytochem Anal* 22(6):532–540
- Willmot FC, Robertson GW (1920) Senecio disease, or cirrhosis of the liver due to senecio poisoning. *Lancet* 196(5069):848–849
- Xia Q, Zhao Y, Von Tungeln LS, Doerge DR, Lin G, Cai L, Fu PP (2013) Pyrrolizidine alkaloid-derived DNA adducts as a common biological biomarker of pyrrolizidine alkaloid-induced tumorigenicity. *Chem Res Toxicol* 26(9):1384–1396
- Xia Q, He X, Ma L, Chen SJ, Fu pp. (2018) Pyrrolizidine alkaloid secondary pyrrolic metabolites construct multiple activation pathways leading to DNA adduct formation and potential liver tumor initiation. *Chem Res Toxicol* 31(7):619–628
- Yang MB, Ruan JQ, Gao H, Li N, Ma J, Xue JY, Ye Y, Fu PP, Wang JY, Lin G (2017) First evidence of pyrrolizidine alkaloid N-oxide-induced hepatic sinusoidal obstruction syndrome in humans. *Arch Toxicol* 91(12):3913–3925
- Yang MB, Ma J, Ruan JQ, Ye Y, Fu PP, Lin G (2019) Intestinal and hepatic biotransformation of pyrrolizidine alkaloid N-oxides to toxic pyrrolizidine alkaloids. *Arch Toxicol* 93(8):2197–2209
- Yang MB, Ma J, Ruan J, Zhang C, Ye Y, Fu PP, Lin G (2020) Absorption difference between hepatotoxic pyrrolizidine alkaloids and their N-oxides – mechanism and its potential toxic impact. *J Ethnopharmacol* 249:112421. <https://doi.org/10.1016/j.jep.2019.112421>
- Zhao Y, Xia QS, Yin JJ, Lin G, Fu pp. (2011) Photoirradiation of dehydropyrrolizidine alkaloids–formation of reactive oxygen species and induction of lipid peroxidation. *Toxicol Lett* 205(3):302–309
- Zhao Y, Xia Q, Gamboa da Costa G, Yu H, Cai L, Fu pp. (2012) Full structure assignments of pyrrolizidine alkaloid DNA adducts and mechanism of tumor initiation. *Chem Res Toxicol* 25(9):1985–1996
- Zhu L, Xue J, Xia Q, Fu PP, Lin G (2017) The long persistence of pyrrolizidine alkaloid-derived DNA adducts in vivo: kinetic study following single and multiple exposures in male ICR mice. *Arch Toxicol* 91(2):949–965
- Zhu L, Wang Z, Wong L, He Y, Zhao Z, Ye Y, Fu PP, Lin G (2018) Contamination of hepatotoxic pyrrolizidine alkaloids in retail honey in China. *Food Control* 85:484–494
- Zhu L, Zhang CY, Li DP, Chen HB, Ma J, Gao H, Ye Y, Wang JY, Fu PP, Lin G (2020) Tu-San-Qi (*Gynura japonica*): the culprit behind pyrrolizidine alkaloid-induced liver injury in China. *Acta Pharmacol Sin*. <https://doi.org/10.1038/s41401-020-00553-9>
- Zhuge YZ, Liu YL, Xie WF, Zou XP, Xu JM, Wang JY, Chinese Society of Gastroenterology Committee of Hepatobiliary Disease (2019) Expert consensus on the clinical management of pyrrolizidine alkaloid-induced hepatic sinusoidal obstruction syndrome. *J Gastroenterol Hepatol* 34(4):634–642

Publisher's Note Springer Nature remains neutral with regard to jurisdictional claims in published maps and institutional affiliations.